



# Comparison of dehydriding kinetics between pure LaNi<sub>5</sub> and its substituted systems

Xue-Hui An, Lei-Gang Li, Jie-Yu Zhang, Qian Li\*

Shanghai Key Laboratory of Modern Metallurgy & Materials Processing, Shanghai University, Shanghai 200072, China

## ARTICLE INFO

### Article history:

Received 21 January 2011

Received in revised form 11 July 2011

Accepted 4 September 2011

Available online 10 September 2011

### Keywords:

Metal hydrides

Gas–solid reactions

Kinetics

## ABSTRACT

The kinetic mechanisms of dehydriding reaction in La<sub>0.8</sub>M<sub>0.2</sub>Ni<sub>5</sub> and LaNi<sub>4.5</sub>T<sub>0.5</sub> were comparatively investigated by the Chou model and the first order model, and the former was superior to the latter from the comparison of theoretical calculated results and experimental data. According to the characteristic time ( $t_c$ ) in the Chou model, substituting La ( $t_c = 71.36$  s) with Ce ( $t_c = 35.64$  s), Nd ( $t_c = 30.82$  s) and Pr ( $t_c = 28.86$  s) increased the dehydriding reaction rate, but partial substitution of Ni ( $t_c = 71.36$  s) with Co ( $t_c = 102.29$  s), Fe ( $t_c = 116.70$  s) and Cu ( $t_c = 120.62$  s) decreased the hydrogen desorption reaction rate. The Chou model was also used to discuss the effect of different amount of Ni substituted with Fe and Co. The dehydriding reaction rates of La(Ni<sub>1-x</sub>Fe<sub>x</sub>)<sub>5</sub> increased with  $x$  leveling from 0 to 0.20 but decreased with  $x$  increasing from 0.20 to 0.30, while that of LaNi<sub>5-y</sub>Co<sub>y</sub> decreased with increasing the amount of Co from 0 to 3.00. In addition, the Chou model was successfully applied to predicting the kinetic properties of LaNi<sub>4.8</sub>Sn<sub>0.2</sub> at 40 °C and 60 °C, which exhibited an excellent agreement with the experimental data.

© 2011 Elsevier B.V. All rights reserved.

## 1. Introduction

LaNi<sub>5</sub>-type hydrogen storage alloys have been extensively studied for its favorable hydriding/dehydriding (H/D) characteristics [1,2], but its disadvantages are short cycling life, easy pulverization and high cost. It is well known that element substitution is an effective way to improve thermodynamics and kinetics of hydrogen storage alloys. Partial substitution of La by Pr, Nd and Ce can obviously improve the cycling life, decrease the hysteresis and lower the thermodynamic stability [3,4]. Partial substitution of Ni with Fe, Al, Cu and Mn could enhance the pulverization resistance, increase the hydrogen storage capacity and reduce the plateau pressure [5,6].

Revealing the H/D kinetic mechanism is significant to the practical application. The kinetic mechanism of LaNi<sub>5</sub>-type hydrogen storage alloys has been extensively investigated by model fitting method, however, different researchers obtained different conclusions. For example, Smith and Goudy [7] reported that the rate-controlling step of dehydriding process was chemical reaction at the  $\alpha$ - $\beta$  interface of LaNi<sub>5-x</sub>Co<sub>x</sub> ( $x=0, 1.00, 2.00, 3.00$ ) alloys using the shrinking core model. Muthukumar et al. [8] found that the kinetics of LaNi<sub>5</sub>, LaNi<sub>4.7</sub>Al<sub>0.3</sub> and LaNi<sub>4.91</sub>Sn<sub>0.15</sub> were better illustrated by the Jander model than the first order model. Sato et al. [9] obtained that diffusion was the rate-controlling step for the hydrogen desorption reaction of LaNi<sub>4.7</sub>Sn<sub>0.3</sub> using a

spherical model. Dhaou et al. [10] concluded that LaNi<sub>4.75</sub>Fe<sub>0.25</sub> had the slowest dehydriding reaction rate above 303 K among LaNi<sub>5</sub>, LaNi<sub>4.85</sub>Al<sub>0.15</sub> and LaNi<sub>4.75</sub>Fe<sub>0.25</sub>. In our previous work, the influence of temperature, pressure and Al content on the hydriding reaction kinetic mechanism of LaNi<sub>5-x</sub>Al<sub>x</sub> ( $0 \leq x \leq 1.00$ ) was clarified using the Chou model [11]. Although numerous kinetic models were applied to elucidate the kinetic mechanism of LaNi<sub>5</sub>-type hydrogen storage alloys, some of which do not provide an intuitive expression for discussion and no consistent conclusion has been obtained yet.

In the present work, the dehydriding reaction rate of LaNi<sub>5</sub> and its substituted systems were compared, and the experimental data summarized from literatures [7,12–15]. The influences of substituting La or Ni with different elements were comparatively studied by the Chou model and the first order model. Then, the effects of different amounts of Fe and Co substituted for Ni and temperature on the dehydriding reaction kinetics of the LaNi<sub>4.8</sub>Sn<sub>0.2</sub> were analyzed using the Chou model.

## 2. Models

### 2.1. Chou model

Chou and Xu [16] supposed that the particles were hydride spheres with the same diameter and density, and the H/D reaction consisted of seven steps, of which diffusion or surface penetration was the rate-controlling step in most cases. The derivation of mathematical expression for each step was detailedly described in Ref.

\* Corresponding author. Tel.: +86 21 56338065; fax: +86 21 56338065.  
E-mail address: [qian246@hotmail.com](mailto:qian246@hotmail.com) (Q. Li).

[16]. It should be noted that the Chou model is expressed as explicit functions of the reacted fraction  $\xi$  and time  $t$ , which make it easy to compare the reaction rates through a specific value of the characteristic time  $t_c$ . More importantly, the Chou model can be used to analyze as well as predict the kinetic mechanism of H/D reaction.

According to the Chou model, when the rate-controlling step is surface penetration, the expression is written as

$$\xi = 1 - \left[ \frac{K_{sp}^0 \sqrt{K_{pa}^0 K_{ca}^0} (\sqrt{P_H} - \sqrt{P_{eq}}) \exp(-E_{v(sp)}/RT)}{R_0^2 \nu_m} \right]^3 \quad (1)$$

where  $E_{v(sp)}$  (J/mol) is the activation energy;  $P_H$  (MPa) is partial pressure of hydrogen in gas phase;  $P_{eq}$  (MPa) is the hydrogen partial pressure in equilibrium with hydride;  $K_{pa}^0$ ,  $K_{ca}^0$ ,  $K_{sp}^0$  and  $D$  are constant;  $\nu_m$  is coefficient depending on substance and reaction;  $R_0$  is the radius of the particle;  $R$  is the gas constant;  $T$  (K) is the reaction temperature.

Define  $t_c = 1 / (K_{sp}^0 \sqrt{K_{pa}^0 K_{ca}^0} (\sqrt{P_H} - \sqrt{P_{eq}}) \exp(-E_{v(sp)}/RT) / (R_0^2 \nu_m))$ , then Eq. (1) can be expressed as

$$\xi = 1 - \left(1 - \frac{t}{t_c}\right)^3 \quad (2)$$

when  $t = t_c$ ,  $\xi = 1$ . Obviously, the physical meaning of  $t_c$  is the required time for the H/D reaction to be completed. The smaller the value of  $t_c$  is, the faster the reaction processes. Eq. (2) is used to clarify the kinetic mechanism in this work.

## 2.2. First order model

Arvami [17–19], Johnson and Mehl [20] made great contributions to analyze the process of nucleation and growth. Johnson and Mehl began their work with discussing the reason why reactions in metallic systems were different from chemical reactions. Then, they made four assumptions, which are (i) the reaction proceeds by nucleation and growth; (ii) the rate of nucleation ( $N_v$ ) and the rate of radial growth ( $G$ ) are constant throughout the reaction; (iii) the nucleation is random and (iv) the reaction product is spheres when no impingement occurs during growth. The equation is expressed as

$$\xi = 1 - \exp\left(-\frac{\pi}{3} N_v G^3 t^4\right) \quad (3)$$

Eq. (3) depicts a sigmoid shape curve as  $\xi$  increases from 0 to 1. However, Arvami did not totally agree with Johnson and Mehl, and later, he proposed a function, expressed as Eq. (4)

$$\xi = 1 - \exp(-Bt^K) \quad (4)$$

Generally, Eq. (4) is written as

$$\xi = 1 - \exp(-kt^n) \quad \text{or} \quad \xi = 1 - \exp((-kt)^n) \quad (5)$$

When  $n = 1$ , Eq. (5) become

$$\xi = 1 - \exp(-kt) \quad (6)$$

In most cases, Eq. (6) is described as

$$kt = -\ln(1 - \xi) \quad (7)$$

where  $K$  and  $n$  is the reaction order and its value identifies the nature of the rate-controlling process;  $B$  and  $k$  is the rate constant, which depends on temperature.

Eqs. (6) and (7) are the expression of the first order model, however, Eq. (7) is often used to analyze the kinetic mechanism. Make plot of  $-\ln(1 - \xi)$  vs.  $t$ , the rate constant  $k$  can be obtained, which is often used to analyze the thermally activated process described by Arrhenius relationship. In this paper, Eq. (7) is used to calculate the experimental data.

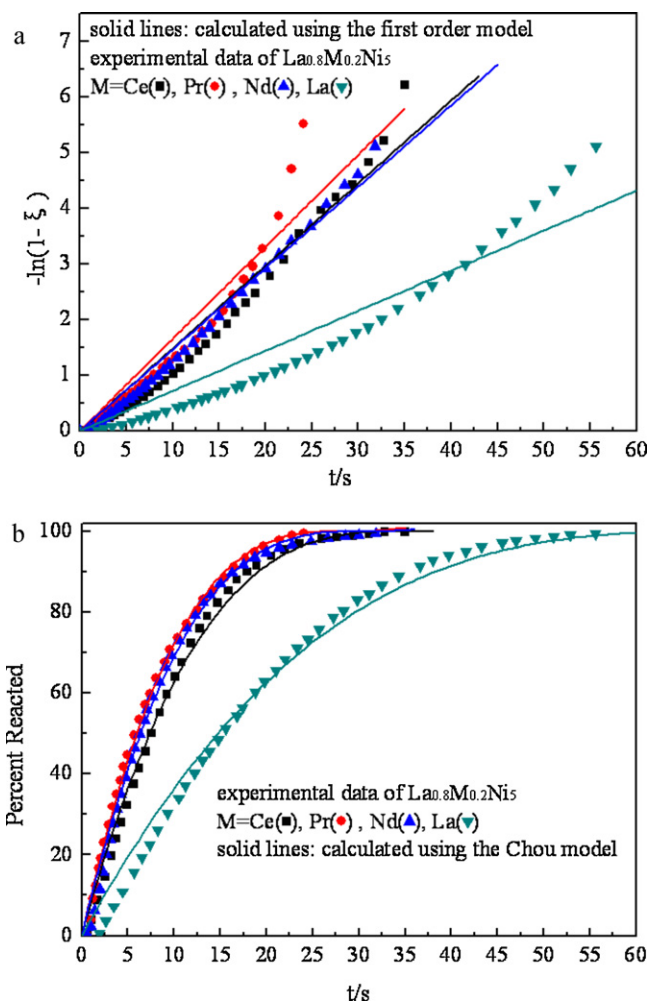


Fig. 1. The dehydrogenation kinetics of  $\text{La}_{0.8}\text{M}_{0.2}\text{Ni}_5$  (M = La, Ce, Pr, Nd) [12] together with the calculated using the first order model (a) and the Chou model (b).

## 3. Results and discussion

### 3.1. The effect of substituting La with Ce, Pr and Nd on the dehydrogenation kinetics of $\text{LaNi}_5$

Clay et al. [12] investigated the effect of partial substitution of La with Ce, Pr and Nd (marked as  $\text{La}_{0.8}\text{M}_{0.2}\text{Ni}_5$  (M = La, Ce, Pr, Nd)) on the hydrogen storage properties of  $\text{LaNi}_5$ . The hydrogen desorption reaction kinetics were measured at 25 °C and  $P_{eq}/P_{op} = 2$  (the ratio of the equilibrium plateau pressure to the opposing pressure was equal to 2), which were analyzed by the Chou model and the first order model.

The experimental data of  $\text{La}_{0.8}\text{M}_{0.2}\text{Ni}_5$  are presented in Fig. 1. Curves in Fig. 1(a) are calculated using the first order model, i.e. Eq.(7), while the curves calculated from the Chou model are shown in Fig. 1(b), which shows the plot of percent hydrogen desorbed vs. time. As clearly seen from Fig. 1(a), the theoretical calculated curves show a large deviation from the experimental data. Clay et al. [12] declared that none of the plots calculated from the first order model are strictly linear and this might be caused by different rate-controlling steps throughout reaction. However, from Fig. 1(b), it can be seen that the calculated curves show an excellent agreement with experimental data. The parameters calculated from these two models are listed in Table 1. The  $r^2$  of the linear regression equations of the first order model is 0.96, 0.98, 0.95 and 0.95 for  $\text{La}_{0.8}\text{Ce}_{0.2}\text{Ni}_5$ ,  $\text{La}_{0.8}\text{Nd}_{0.2}\text{Ni}_5$ ,  $\text{La}_{0.8}\text{Pr}_{0.2}\text{Ni}_5$  and  $\text{LaNi}_5$ ,

**Table 1**

The parameters ( $t_c$ ,  $r^2$  or  $k$ ) calculated using the Chou model and the first order model.

Sample	Chou model		First order model	
	$t_c$ (s)	$r^2$	$k$ ( $\times 10^{-2}$ )	$r^2$
La <sub>0.8</sub> Ce <sub>0.2</sub> Ni <sub>5</sub>	35.64	0.99	14.84	0.96
La <sub>0.8</sub> Nd <sub>0.2</sub> Ni <sub>5</sub>	30.82	0.99	14.63	0.98
La <sub>0.8</sub> Pr <sub>0.2</sub> Ni <sub>5</sub>	28.86	0.99	16.56	0.95
LaNi <sub>5</sub>	71.36	0.99	7.59	0.95
LaNi <sub>4.5</sub> Co <sub>0.5</sub>	102.29	0.99	4.86	0.94
LaNi <sub>4.5</sub> Fe <sub>0.5</sub>	116.70	0.99	4.17	0.95
LaNi <sub>4.5</sub> Cu <sub>0.5</sub>	120.62	0.99	4.12	0.94

respectively. However, all the  $r^2$  of La<sub>0.8</sub>M<sub>0.2</sub>Ni<sub>5</sub> calculated using the Chou model is more than 0.99. Therefore, the Chou model is superior to the first order model in analyzing the dehydrogenation reaction kinetic mechanism, and surface penetration is the rate-controlling step.

As listed in Table 1, the rate constant  $k$  is increased, i.e. the reaction rate is increased, as La is substituted by Ce, Pr and Nd. The same conclusion is obtained from the Chou model. The characteristic times of LaNi<sub>5</sub>, La<sub>0.8</sub>Ce<sub>0.2</sub>Ni<sub>5</sub>, La<sub>0.8</sub>Nd<sub>0.2</sub>Ni<sub>5</sub> and La<sub>0.8</sub>Pr<sub>0.2</sub>Ni<sub>5</sub> are 71.36 s, 35.64 s, 30.82 s and 28.86 s, respectively, indicating that the dehydrogenation reaction rate of LaNi<sub>5</sub> is doubled after partial substitution, and the order is LaNi<sub>5</sub> < La<sub>0.8</sub>Ce<sub>0.2</sub>Ni<sub>5</sub> < La<sub>0.8</sub>Nd<sub>0.2</sub>Ni<sub>5</sub> < La<sub>0.8</sub>Pr<sub>0.2</sub>Ni<sub>5</sub>. The reason why substitutions on La made the reaction rate increased is that the dehydrogenation reaction rate is inversely proportional to hydride stability. Partial substitution of La by Pr, Nd and Ce can obviously increase the plateau pressure [3,4], and thus lower the thermodynamic stability, so the dehydrogenation reaction rate becomes larger. In Ref. [12], the author also reported that LaNi<sub>5</sub> has the lower plateau pressure than any other alloys, therefore, the kinetics is slowest.

### 3.2. The effect of substituting Ni with Cu, Co and Fe on the dehydrogenation kinetics of LaNi<sub>5</sub>

Zarynow et al. [13] investigated the effect of partial substitution of Ni with Cu, Co and Fe on the hydrogen storage properties of LaNi<sub>5</sub> at 25 °C and  $P_{eq}/P_{op} = 2$ . They reported that the dehydrogenation reaction kinetics of LaNi<sub>4.5</sub>T<sub>0.5</sub> (T = Ni, Cu, Co, Fe) was better analyzed by the first order model than the zero and second order models, even though the first order model cannot well describe the experimental data. It should be noted that their goal was not to reveal the kinetic mechanism, but to discuss the effect of partial substitution of Ni with Cu, Co and Fe on hydrogen storage properties of LaNi<sub>5</sub>. Therefore, the kinetic mechanism was clarified in the present work.

Fig. 2(a) presents the calculated curves from the first order model, which shows that a large deviation exists between the calculated results and the experimental data. However, the curves calculated using the Chou model exhibit an excellent accordance with the experimental data, as shown in Fig. 2(b), which presents plots of percent hydrogen desorbed vs. time. In Table 1, the  $r^2$  of LaNi<sub>5</sub>, LaNi<sub>4.5</sub>Co<sub>0.5</sub>, LaNi<sub>4.5</sub>Fe<sub>0.5</sub> and LaNi<sub>4.5</sub>Cu<sub>0.5</sub> is 0.95, 0.94, 0.95 and 0.94 for the first order model, respectively. However, the  $r^2$  of LaNi<sub>4.5</sub>T<sub>0.5</sub> calculated from the Chou model is more than 0.99. Therefore, we can conclude that the Chou model is better than the first order model in analyzing the hydrogen desorption reaction kinetic mechanism. Surface penetration is the rate-controlling step.

According to Table 1, the rate constant of LaNi<sub>5</sub>, LaNi<sub>4.5</sub>Co<sub>0.5</sub>, LaNi<sub>4.5</sub>Fe<sub>0.5</sub> and LaNi<sub>4.5</sub>Cu<sub>0.5</sub> are 7.59, 4.86, 4.17 and 4.12, respectively, denoting that partial substitution of Ni with Co, Fe and Cu reduces the dehydrogenation reaction rate. This conclusion is also obtained from the Chou model. The characteristic times of LaNi<sub>5</sub>, LaNi<sub>4.5</sub>Co<sub>0.5</sub>, LaNi<sub>4.5</sub>Fe<sub>0.5</sub> and LaNi<sub>4.5</sub>Cu<sub>0.5</sub> are corresponding to 71.36 s, 102.29 s, 116.70 s and 120.62 s, indicating that the reaction

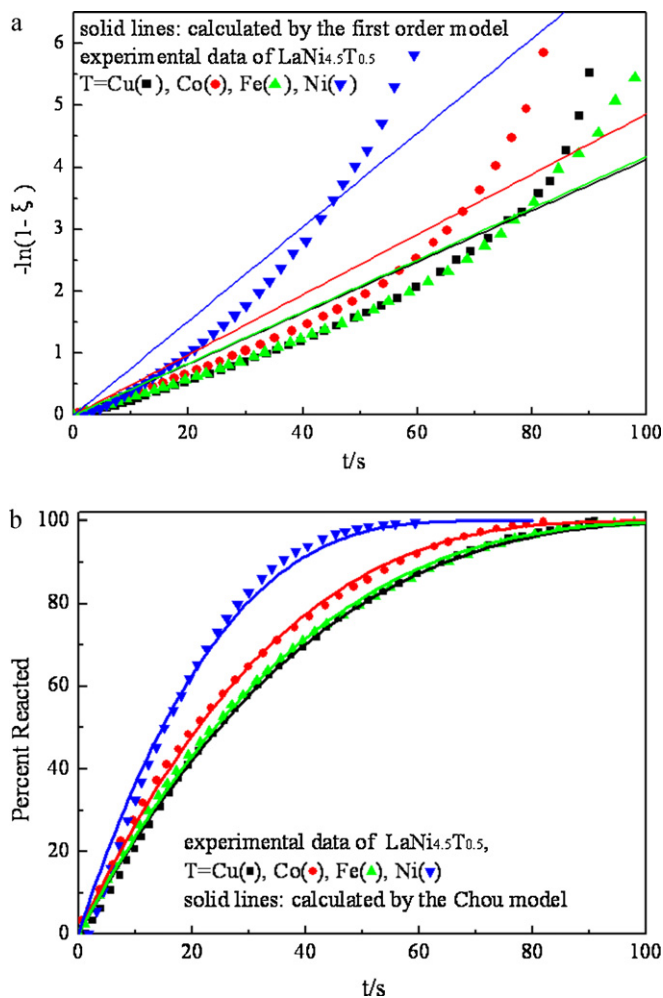


**Fig. 2.** The dehydrogenation kinetics of LaNi<sub>4.5</sub>T<sub>0.5</sub> (T = Ni, Fe, Co, Cu) [13] together with calculated results using the first order model (a) and the Chou model (b).

rate order follows LaNi<sub>4.5</sub>Cu<sub>0.5</sub> < LaNi<sub>4.5</sub>Fe<sub>0.5</sub> < LaNi<sub>4.5</sub>Co<sub>0.5</sub> < LaNi<sub>5</sub>. Substitution of Ni with other elements lowers the plateau pressure [5–7] and increases the thermodynamic stability, which makes the reaction rate decreased, therefore, LaNi<sub>5</sub> has the largest dehydrogenation reaction rate.

### 3.3. The effect of substituting Ni with different amounts of Fe and Co on the dehydrogenation kinetics of LaNi<sub>5</sub>

Partial substitution of Ni with some third transition elements was extensively studied because it can reduce the plateau pressure, and thus affect the kinetics. However, the influence on kinetic mechanism is different among different elements. The effect of different substituted elements with equal amount has been discussed in the Section 3.2 as well as Ref. [6], therefore, it is significant to clarify the effect of different substituted amounts with the same element.

Pandey et al. [14] studied the hydrogen storage properties of La(Ni<sub>1-x</sub>Fe<sub>x</sub>)<sub>5</sub> ( $x = 0, 0.05, 0.10, 0.20, 0.25, 0.30$ ) alloys. They reported that the dehydrogenation reaction rate of La(Ni<sub>0.8</sub>Fe<sub>0.2</sub>)<sub>5</sub> is larger than any other alloys, but no model was used to analyze their kinetic mechanisms. The hydrogen desorption kinetic curves were obtained using a Sievert's type apparatus with the volume displacement method, as shown in Fig. 3(a), which presents plot of

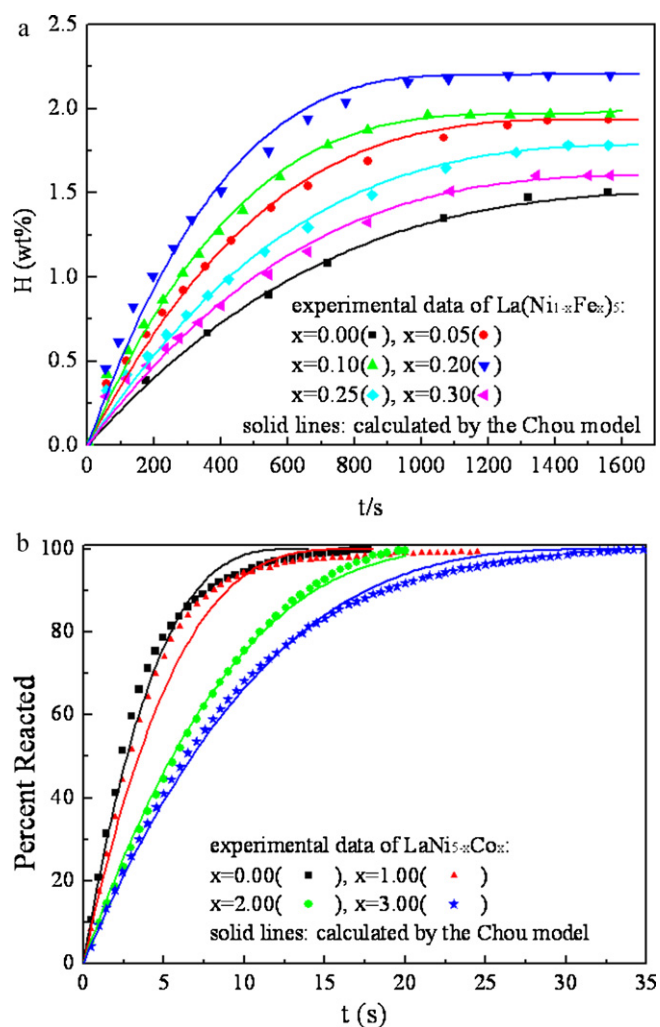


**Fig. 3.** The dehydrogenating kinetics of the  $\text{La}(\text{Ni}_{1-x}\text{Fe}_x)_5$  [14] (a) and  $\text{LaNi}_{5-y}\text{Co}_y$  [7] (b) alloys together with calculated results using the Chou model.

the hydrogen amount vs. time. The relationship between reacted fraction and hydrogen amount can be written as

$$\xi = \frac{\Delta m}{\Delta m_{\max}} = \frac{\Delta m/m_0}{\Delta m_{\max}/m_0} \quad (8)$$

where  $\Delta m$  is the reacted amount,  $\Delta m_0$  is the initial weight of the sample,  $\Delta m/\Delta m_0$  is the percentage of the reacted amount, and  $\Delta m_{\max}$  is the maximum reacted amount.

The calculated curves of  $\text{La}(\text{Ni}_{1-x}\text{Fe}_x)_5$  using the Chou model are shown in Fig. 3(a), which agreed well with the experimental data. The  $r^2$  of the linear regression equations is calculated to be 0.98, suggesting that the kinetic mechanisms of  $\text{La}(\text{Ni}_{1-x}\text{Fe}_x)_5$  can be well clarified by the Chou model and the rate-controlling step is surface penetration. For  $\text{La}(\text{Ni}_{1-x}\text{Fe}_x)_5$ , when  $x$  takes values of 0, 0.05, 0.10, 0.20, 0.25 and 0.30, the characteristic times are 2022.06 s, 1518.69 s, 1305.61 s, 1184.12 s, 1769.99 s and 1802.67 s, respectively, which indicate that the hydrogen desorption reaction rates initially increase with increasing  $x$  at the range of 0–0.20 and then decrease with further increasing  $x$  from 0.20 to 0.30, but the dehydrogenating reaction rate of  $\text{LaNi}_5$  is the smallest among the alloys, which may be ascribed to the crystal structure. The unit cell volume of  $\text{La}(\text{Ni}_{0.8}\text{Fe}_{0.2})_5$  is larger than any other alloys, so the hydrogen desorption reaction rate is the largest [14].

Smith and Goudy [7] investigated the kinetics of  $\text{LaNi}_{5-y}\text{Co}_y$  ( $y=0, 1.00, 2.00, 3.00$ ) hydride system at 60 °C and  $P_{\text{eq}}/P_{\text{op}}=3$  using the shrinking core model. They reported that the dehydrogenating

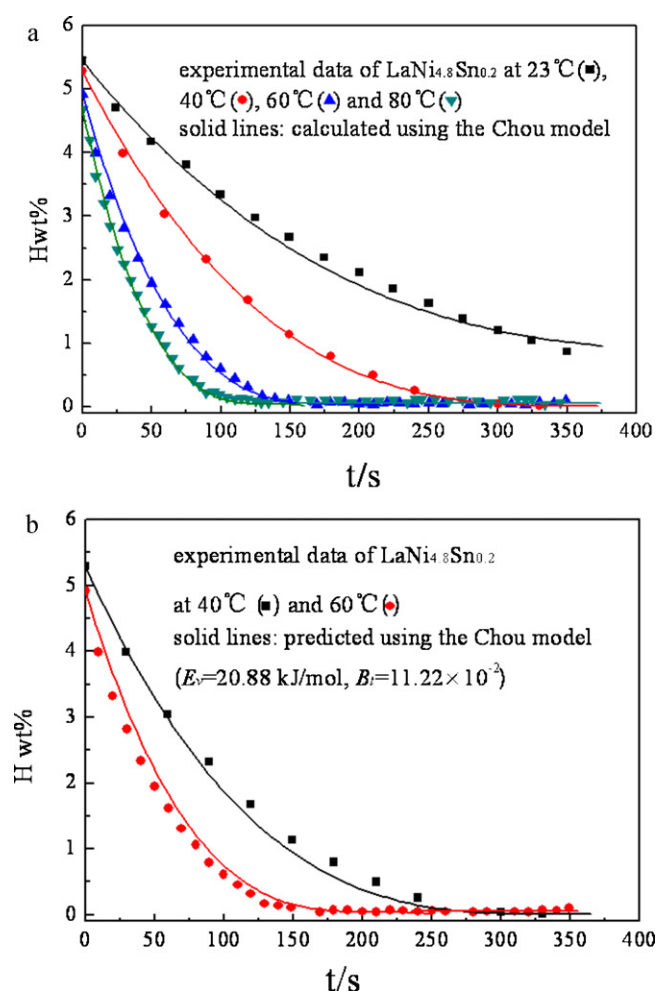


**Fig. 4.** The dehydrogenating kinetics of  $\text{LaNi}_{4.8}\text{Sn}_{0.2}$  [15] at different temperatures together with results calculated (a) and predicted (b) by the Chou model.

reaction rate is reduced by the substitution, and their experimental results are shown in Fig. 3(b), which gives the plot of percent hydrogen desorbed vs. time. The hydrogen desorption reaction kinetics of  $\text{LaNi}_{5-y}\text{Co}_y$  was interpreted using the Chou model, as curves shown in Fig. 3(b), which shows a good agreement with the experimental data. The  $r^2$  is calculated to be 0.99, which means that the kinetic mechanisms of  $\text{LaNi}_{5-y}\text{Co}_y$  can be well described by the Chou model and surface penetration is the rate-controlling step. The characteristic times of  $\text{LaNi}_5$ ,  $\text{LaNi}_4\text{Co}$ ,  $\text{LaNi}_3\text{Co}_2$  and  $\text{LaNi}_2\text{Co}_3$  are corresponding to 13.08 s, 16.60 s, 26.77 s and 32.73 s, indicating that the dehydrogenating reaction rate is decreased by the substitution of Ni with Co and the reaction rate becomes smaller and smaller with  $y$  increasing from 0 to 3.00. The reason is that the more content of Ni substituted by Co, the hydride becomes more stable [7].

### 3.4. The effect of temperature on dehydrogenating kinetics of $\text{LaNi}_{4.8}\text{Sn}_{0.2}$

The H/D kinetics of  $\text{LaNi}_{4.8}\text{Sn}_{0.2}$  at different temperatures (23 °C, 40 °C, 60 °C, 80 °C) were investigated by Laurencelle et al. [15]. In this paper, the experimental data are analyzed, the activation energy is calculated and the kinetic behaviors at 40 °C and 60 °C are predicted using the Chou model. The experimental data and the calculated results are shown in Fig. 4, which presents plots of the hydrogen amount vs. time.

Fig. 4(a) exhibits the results calculated by the Chou model, which agree well with the experimental data. The  $r^2$  of the linear



regression equation is 0.99, and the rate-controlling step is surface penetration. When the temperatures are 23 °C, 40 °C, 60 °C and 80 °C, the characteristic times are 514.88 s, 370.52 s, 187.16 s and 137.61 s, respectively, suggesting that the dehydriding reaction rate becomes faster with increasing the temperature.

As mentioned in Section 2.1, the Chou model can be used not only to analyze but to predict the H/D reaction process. During the whole experimental process, the partial pressure of hydrogen is assumed to be fixed. Define  $B_t$  as a coefficient, which is expressed by  $B_t = (R_0^2 \nu_m) / (K_{sp}^0 \sqrt{K_{pa}^0 K_{ca}^0} (\sqrt{P_H} - \sqrt{P_{eq}}))$ . Substituting  $B_t$  into Eq. (1), yields

$$\xi = 1 - \left[ 1 - \exp\left(\frac{-E_{V(sp)}}{RT}\right) \cdot \frac{t}{B_t} \right]^3 \quad (9)$$

To predict the kinetic behavior, it is necessary to calculate the activation energy ( $E_{V(sp)}$ ) and the coefficient ( $B_t$ ) first. Then, substituting the specific values of  $E_{V(sp)}$  and  $B_t$  into Eq. (9), the kinetic curves can be predicted. Take  $\text{LaNi}_{4.8}\text{Sn}_{0.2}$  for example, using Eq. (9), the  $E_{V(sp)}$  and  $B_t$  are calculated to be 20.88 kJ/mol and  $11.22 \times 10^{-2}$ , respectively, at 23 °C and 80 °C. The value of  $E_{V(sp)}$  is close to that reported in literature [15], 23.50 kJ/mol. Substituting the values of  $E_{V(sp)}$  and  $B_t$  into Eq. (9), the dehydriding kinetics of  $\text{LaNi}_{4.8}\text{Sn}_{0.2}$  at 40 °C and 60 °C are predicted, as shown in Fig. 4(b), from which it can be seen that the predicted curves are in well accordance with the experimental data.

#### 4. Conclusions

In this work, the dehydriding reaction rate of  $\text{LaNi}_5$  and its sub-systems were compared by the method of kinetic modeling. The dehydriding kinetics of  $\text{La}_{0.8}\text{M}_{0.2}\text{Ni}_5$  and  $\text{LaNi}_{4.5}\text{To}_{0.5}$  were better illustrated by the Chou model than by the first order model. When La was substituted with Ce, Nd and Pr, the dehydriding reaction rate of  $\text{LaNi}_5$  is smallest. However, for partial substitution of Ni with Co, Fe and Cu,  $\text{LaNi}_5$  has the largest hydrogen desorption reaction rate. The hydrogen desorption kinetics of  $\text{LaNi}_{4.8}\text{Sn}_{0.2}$  was increased with increasing the temperature, and the predicted kinetic curves

at 40 °C and 60 °C were well agreed with the experimental data. For the  $\text{LaNi}_5$ -based hydrogen storage alloys studied in this work, surface penetration is the rate-controlling step.

#### Acknowledgements

The authors gratefully acknowledge the financial supports from the National Natural Science Foundation of China (50804029 and 50974084), Science and Technology Commission of Shanghai Municipality (10195802000) and the Program for Changjiang Scholars Innovative Research Team in University (IRT0739).

#### References

- [1] E.M<sup>ac</sup>A. Gray, T.P. Blach, M.P. Pitt, D.J. Cookson, J. Alloys Compd. 509 (2011) 1630–1635.
- [2] J. Cieslik, P. Kula, R. Sato, J. Alloys Compd. 509 (2011) 3972–3977.
- [3] X.X. Yuan, H.S. Liu, Z.F. Ma, N.X. Xu, J. Alloys Compd. 359 (2003) 300–306.
- [4] R. Ngameni, N. Mbemba, S.A. Grigoriev, P. Millet, Int. J. Hydrogen Energy 36 (2011) 4178–4184.
- [5] S.L. Li, P. Wang, W. Chen, G. Luo, X.B. Han, D.M. Chen, K. Yang, Int. J. Hydrogen Energy 35 (2010) 12391–12397.
- [6] S.L. Li, P. Wang, W. Chen, G. Luo, D.M. Chen, K. Yang, J. Alloys Compd. 485 (2009) 867–871.
- [7] G. Smith, A.J. Goudy, J. Alloys Compd. 316 (2001) 93–98.
- [8] P. Muthukumar, A. Satheesh, M. Linder, R. Mertz, M. Groll, Int. J. Hydrogen Energy 34 (2009) 7253–7262.
- [9] M. Sato, M. Stange, V.A. Yartys, J. Alloys Compd. 396 (2005) 197–201.
- [10] H. Dhaou, F. Askri, M.B. Salah, A. Jemni, S.B. Nasrallah, J. Lamloumi, Int. J. Hydrogen Energy 32 (2007) 576–587.
- [11] X.H. An, Y.B. Pan, Q. Luo, X. Zhang, J.Y. Zhang, Q. Li, J. Alloys Compd. 506 (2010) 63–69.
- [12] K.R. Clay, A.J. Goudy, R.G. Schweibenz, A. Zarynow, J. Less-Common Met. 166 (1990) 153–162.
- [13] A. Zarynow, A.J. Goudy, R.G. Schweibenz, K.R. Clay, J. Less-Common Met. 172–174 (1991) 1009–1017.
- [14] S.K. Pandey, A. Srivastava, O.N. Srivastava, Int. J. Hydrogen Energy 32 (2007) 2461–2465.
- [15] F. Laurencelle, Z. Dehouche, J. Goyette, J. Alloys Compd. 424 (2006) 266–271.
- [16] K.C. Chou, K.D. Xu, Intermetallics 15 (2007) 767–777.
- [17] M. Arvami, J. Chem. Phys. 7 (1939) 1103–1113.
- [18] M. Arvami, J. Chem. Phys. 8 (1940) 212–225.
- [19] M. Arvami, Granulation, J. Chem. Phys. 9 (1941) 177–185.
- [20] W.A. Johnson, R.F. Mehl, Trans. Am. Inst. Min. (Metall.) Eng. 135 (1939) 416–458.